PHYSICAL REVIEW B **69**, 100403(R) (2004)

# Large and small polaron excitations in $La_{2/3}(Sr/Ca)_{1/3}MnO_3$ films

Ch. Hartinger, F. Mayr, J. Deisenhofer, and A. Loidl
*EP V, Center for Electronic Correlations and Magnetism, Augsburg University, 86159 Augsburg, Germany*

T. Kopp
*EP VI, Center for Electronic Correlations and Magnetism, Augsburg University, 86159 Augsburg, Germany*

(Received 3 November 2003; published 8 March 2004)

We present detailed optical measurements of the mid-infrared (MIR) excitations in thin films of $La_{2/3}Sr_{1/3}MnO_3$ (LSMO) and $La_{2/3}Ca_{1/3}MnO_3$ (LCMO) across the magnetic transition. The shape of the excitation at about 0.2 eV in both samples is analyzed in terms of polaron models. We propose to identify the MIR resonance in LSMO as the excitation of large polarons and that in LCMO as a small polaron excitation. A scaling behavior for the low-energy side of the polaronic MIR resonance in LSMO is established.

DOI: 10.1103/PhysRevB.69.100403 PACS number(s): 75.47.Lx, 78.20.Ls, 71.38.−k, 72.80.−r

Historically, polarons were best identified in measurements with charge carriers in nonmetals (e.g., from *F* centers in alkali halides) or doped semiconductors. More recently, the concept of polaronic excitations has again been in the focus of solid-state research with the advent of strongly correlated electronic systems, especially with the discoveries of high-temperature superconductivity and the colossal magnetoresistance in thin films of $La_{2/3}Ca_{1/3}MnO_3$ (LCMO).[1] In both classes of these correlated materials cuprates, and manganites, it is now widely accepted that, in the presence of a strong electron-phonon coupling, polaronic effects have to be considered an important ingredient to understand the complex physical properties of these compounds.[2]

The fingerprints of polarons in the manganites are usually associated with the temperature dependence of high-temperature dc resistivity[3] and the occurrence of a midinfrared (MIR) excitation in the optical conductivity—termed polaron peak in the following—which has been observed by several authors in both single crystalline[4–8] and thin film manganites.[9–11] Though evidence of the signature of polarons in the optical conductivity[12–14] has been reported abundantly, the question whether the charge carriers are rather delocalized (large polarons, LP) or strongly localized in a locally polarized lattice (small polarons, SP) remains still under debate in the case of manganites.

Theoretically, SP and LP have been investigated in several studies[15–17] on doped manganites, but the observed polaron peak has been evaluated mainly in terms of the SP model or through Gaussian or Lorentzian fits for a phenomenological description.[5,18] Kim *et al.* reported on experimental evidence for a LP excitation in polycrystalline LCMO,[6] but unfortunately they did not identify the LP through a fit to the proposed LP model by Emin.[19]

The purpose of this paper is to elucidate the nature of the polaronic charge carriers by comparison of optical spectroscopy measurements in thin films of LCMO and $La_{2/3}Sr_{1/3}MnO_3$ (LSMO). In contrast to single crystals the use of thin films has the advantage of a lower conductivity due to grain boundaries and internal strain. Consequently, screening is effectively reduced—to a level where phonons and polarons are well observable in the optical conductivity, even in the metallic phase. This allows the detailed analysis of polarons from the respective optical data.

We demonstrate that the distinctive shape of the polaron peak in LCMO differs significantly from the one in LSMO allowing to distinguish between SP in LCMO and LP in LSMO. A striking characteristic of the polaron peak in LSMO is the observed scaling behavior for the low-energy side (see Fig. 2). We will confirm this scaling in a weak-coupling evaluation, analogous to that of Tempere and Devreese for *an interacting many-polaron gas*.[20]

As the lattice distortion is of major importance for the effect of charge-carrier localization, the structural differences between LCMO, which is orthorhombically distorted, and LSMO, which reveals a rhombohedral symmetry, represent promising conditions to find distinct regimes of the electron-phonon coupling strength $\alpha$ and, consequently, to distinguish between competing polaronic models.

Thin films have been prepared using a standard pulsed laser deposition technique.[21] They were grown onto single crystalline substrates: LSMO on $(LaAlO_3)_{0.3}(Sr_2AlTaO_5)_{0.7}$ and LCMO on $NdGaO_3$. The typical thin film thickness was between 200 nm and 400 nm. X-ray analysis revealed a rhombohedral structure for LSMO and a preferred growth along the [100] axis. For LCMO an orthorhombic structure was found and the growth direction was [110]. Below room temperature the reflectivities of the sample and the pure substrate were measured using the Fourier-transform spectrometers Bruker IFS 113v and IFS 66v/S, to cover the frequency range from 50 to 40 000 $cm^{-1}$. In addition, the reflectance for frequencies from 10 to 30 $cm^{-1}$ was calculated from the measured complex conductivity data, which were obtained by submillimeter-transmission measurements using a Mach-Zehnder-type interferometer. This setup allows the measurement of both the transmittance and the phase shift of a film on a substrate. The combined data sets were used for a Kramers-Kronig analysis to obtain the optical conductivity $\sigma$, the real part of the complex conductivity.

In Fig. 1 we present $\sigma(\nu)$ for LSMO (upper panel) and LCMO (lower panel) at different temperatures. In the case of LCMO, with a Curie-temperature $T_C = 243$ K, the spectra in the complete frequency range were measured both in the paramagnetic (PM) and in the ferromagnetic (FM) regime.

 

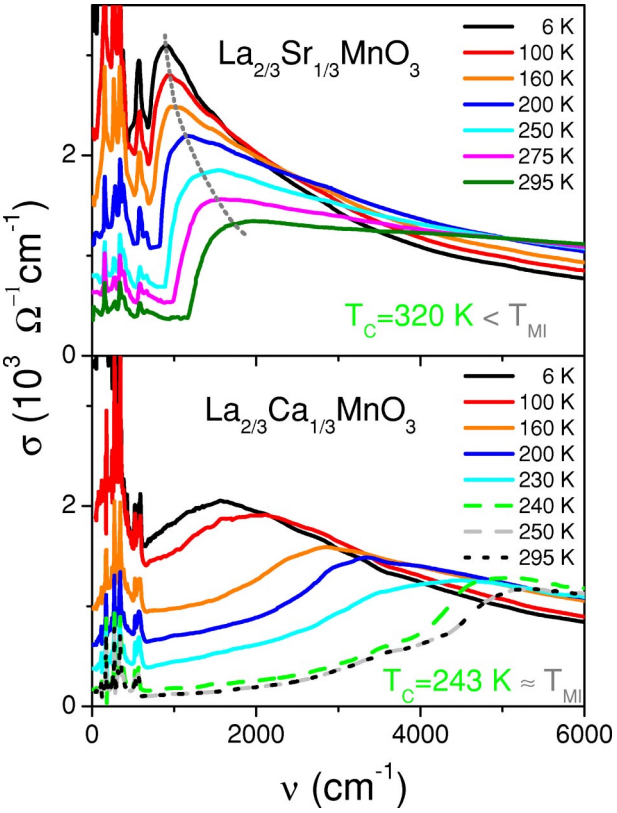


FIG. 1. (Color online) Optical conductivity $\sigma$ for $6\mathrm{K} \leqslant T \leqslant 295$ K. Straight lines represent data in the FM, dashed and dotted lines indicate the PM phase. Upper panel: LSMO ($d=400$ nm). The dotted line is to guide the eyes for the shift of the maximum of the MIR excitation. Lower panel: LCMO ($d=200$ nm).

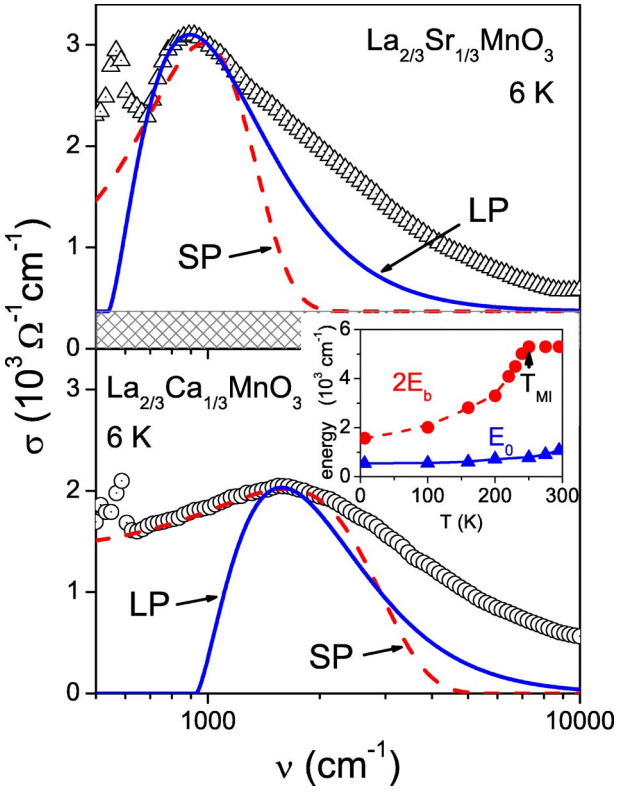


FIG. 2. (Color online) Comparison between fit and experiment for the MIR excitation of LSMO (upper panel) and LCMO (lower panel) at 6 K using a LP model [Eq. (1), solid line] and a SP model [Eq. (2), dashed line]. Inset: polaron binding energy for LCMO ($2E_b$) and for LSMO ($E_0$).

The data for LSMO, as shown in the upper panel of Fig. 1, only cover the FM regimes. We defined $T_C$ as the inflection point and $T_{\mathrm{MI}}$ as the point of the maximum in the dc-resistivity curve.

In LCMO ($d=200$ nm) an almost symmetric but strongly temperature-dependent maximum is observed in the MIR range which suffers a continuous loss of the spectral weight upon increasing the temperature up to $T_C$. Above $T_C$ the temperature dependence is negligible. The maximum moves from 1800 to 5300 $\mathrm{cm}^{-1}$. The loss in spectral weight can be explained in terms of a decreasing carrier mobility.[22] These findings are in agreement with previous studies of Ca-doped manganites.[6,10] For LSMO ($d=400$ nm), in contrast, there is a sharp onset which, along with the asymmetric peak, shifts by approximately a factor of 2 in energy in the range 6 K $< T <$ 295 K. This trend continues up to the insulating phase, where the reflectivity data (not shown) do not change any further.[23]

The prominent feature of the optical spectra, on which we will concentrate in the following, is the distinctly different shape of the polaron peak for LSMO and LCMO. In LSMO the excitation is clearly asymmetric with a steep rise below and a long tail above the peak position, whereas for LCMO a broader hump is visible which is more symmetric about its maximum (compare Fig. 1). A fit with standard single-polaron models highlights the remarkable qualitative differences and allows a preliminary identification (see the respective optical spectra at 6 K in Fig. 2). For the LP fit we took the phenomenological approach by Emin[19] which assumes a photoionization of the charge carriers from self-trapped into free-carrier states. The threshold behavior of the respective optical conductivity

$$\sigma(\omega) = n_p \frac{64}{3} \frac{e^2}{m} \frac{1}{\omega} \frac{(k(\omega)R)^3}{[1+(k(\omega)R)^2]^4} \qquad (1)$$

reproduces the observed upturn at the low-frequency side of the polaron peak. Here, $k(\omega) = \sqrt{2m\hbar(\omega-\omega_0)}/\hbar$, with the temperature-dependent threshold frequency for the absorption $\omega_0 = E_0/\hbar = 2\pi\nu_0$ (see inset of Fig. 2). $E_0$ is interpreted as the energy difference between the localized ground state and the lowest continuum state. The radius of the hydrogenic ground state of the polaron is $R$, the density of polarons is $n_p$, and $m$ is the (effective) mass of the free-carrier states at the band minimum. For $m = 3m_e$ ($m_e$ is the free electron mass) and $\nu_0 = 540$ $\mathrm{cm}^{-1}$, we find $R/a = 0.8$ with the lattice constant $a = 3.88$ Å and $n_p \simeq 4\times10^{21}$ $\mathrm{cm}^{-3}$ at 6 K. We challenge this phenomenological approach below and propose a microscopic modeling.

The SP is interpreted in terms of the Holstein small-polaron theory. It has been proposed to apply an extension of the standard SP optical conductivity formula[24,14] to the low-temperature optical spectroscopy:[25,26]

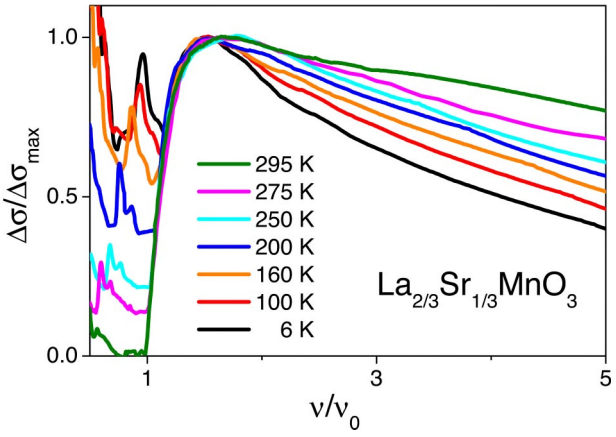


FIG. 3. (Color online) Rescaled optical conductivity of LSMO: $\sigma$ is scaled by the maximum of the resonance, $\nu$ is scaled by the threshold value $\nu_0$ of the onset of the polaronic peak. For $\Delta\sigma$ we subtracted a constant background $\sigma_{bg}=370\ \Omega^{-1}\ \mathrm{cm}^{-1}$ (cf. Fig. 2, Ref. 27). The scaling at the low-frequency slope is nearly independent of the precise value of $\sigma_{bg}$.

$$\sigma(\omega,T)=\sigma(0,T)\frac{\sinh(4E_b\hbar\omega/\Delta^2)}{4E_b\hbar\omega/\Delta^2}e^{-(\hbar\omega)^2/\Delta^2}. \qquad (2)$$

Here $\sigma(0,T)$ is the dc conductivity, $E_b$ is the SP binding energy, $\Delta\equiv 2\sqrt{2E_bE_{\mathrm{vib}}}$, and $E_{\mathrm{vib}}$ is the characteristic vibrational energy being $k_BT$ in the high-temperature regime and $\hbar\omega_{\mathrm{ph}}/2$ at low temperatures ($k_BT<\hbar\omega_{\mathrm{ph}}$, $\omega_{\mathrm{ph}}$ is a phonon frequency). Equation (2) reproduces the broad resonance with a maximum at $2E_b$ (inset of Fig. 2). The *low-energy* SP absorption is well represented by the optical conductivity, Eq. (2). However, one would have to consider the consequences of a high polaron concentration for the absorption in order to understand the slow decay on the *high-frequency* side.

As shown in the inset of Fig. 2, the binding energy $2E_b$ increases towards the metal-insulator transition at $T_{\mathrm{MI}}$, and remains constant above $T_{\mathrm{MI}}$ reflecting the significant role of magnetic interactions in a polaronic system as well as the importance of electron-phonon interactions in the formation of the insulating phase. For LSMO the increase of $E_0$ is weaker corresponding to a weaker electron-phonon interaction. As $T_{\mathrm{MI}}$ is above room temperature for LSMO, $\sigma$ of the insulating phase was not accessible in our experimental setup.

Concerning LCMO, the SP picture is well accepted and both the high-temperature dc resistivity[3] and the rather symmetric line shape close to the maximum of the polaronic excitation suggest that the transport is controlled by incoherent tunneling of SP. For LSMO, the interpretation of the polaron peak in terms of LP is not as obvious. However, an observation related only to LSMO proves to be most valuable in restricting the possible scenarios.

If we scale the frequency by the $T$-dependent threshold value $\nu_0$ and the optical conductivity by its maximum value at the polaron peak, we find a universal low-energy slope independent of temperature (see Fig. 3). This scaling signifies that the low-energy scattering processes which contribute to the absorption for this frequency range relative to $\nu_0$ are of the same origin independent of temperature, related band narrowing, and other energy scales.

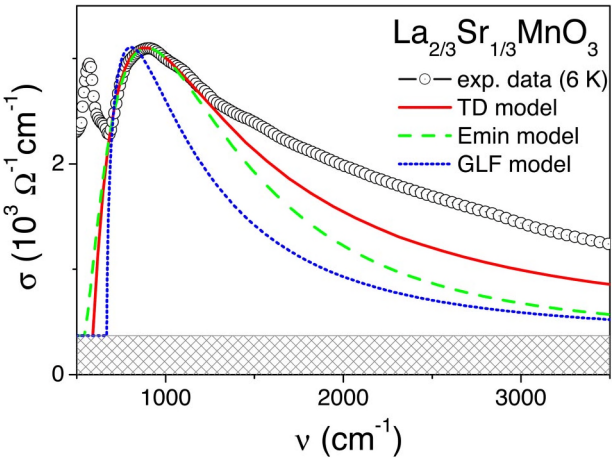


FIG. 4. (Color online) Comparison of the low-temperature MIR optical conductivity to $\sigma(\nu)$ from various model calculations: the solid line refers to the weak-coupling approach of Tempere and Devreese modified for an on-site Hubbard interaction, well approximated by Eq. (4); the dashed line is the result of the phenomenological approach for self-trapped large polarons by Emin, Eq. (1); the dotted curve is the weak-coupling single-polaron result (GLF), Eq. (3).

We challenge that Emin's phenomenological approach is applicable here: (i) it would reproduce the scaling if the dimensionless polaron radius $\varrho\equiv R\sqrt{2mE_0}/\hbar$ were the same for all temperature sets; however, $\varrho$ varies from 0.6 to 0.8, a range of values too large to convincingly support the scaling; (ii) the polaron radius $R/a=0.8$ is small and local lattice effects have to be accounted for; (iii) there is no hole-band minimum available to which the excited charge carriers could scatter. Furthermore, the energy difference from the mobility edge below which the trapped polarons would reside to the hole-band minimum would have to be the threshold frequency. This frequency is about 540 $\mathrm{cm}^{-1}$ at 6 K and is too small for the addressed energy difference.

Consequently the modeling has to be revised as to implement LP's with finite mass and a finite density of charge carriers (Fermi edge). In weak-coupling theory, the generalization of the single-polaron absorption by Gurevich, Lang, and Firsov[28] (GLF) (dotted curve in Fig. 4, $\alpha$ is the coupling strength),

$$\sigma_{\mathrm{GLF}}(\omega)=\alpha n_p\frac{2}{3}\frac{e^2}{m}\frac{1}{\omega_0}\left(\frac{\omega_0}{\omega}\right)^3\sqrt{\frac{\omega}{\omega_0}-1}, \qquad (3)$$

to the situation of many-particle absorption was carried through by Tempere and Devreese for a Coulomb gas.[20] The optical conductivity for a similar approach, which builds on the Hubbard model, is presented by the solid curve in Fig. 4. For the manganites in the ferromagnetic, metallic regime, we take the following standard simplifications for the low-temperature evaluation: (a) only one spin direction prevails (spinless fermions) due to double exchange and strong Hund's coupling; (b) there are two degenerate orbital states

(the two $e_g$ levels); (c) the interaction is represented by the local Hubbard $U$ for two fermions on the same site in two $e_g$ orbital states. We adjust the parameters as follows: the density of charge carriers is $n_p = 6 \times 10^{21}$ cm$^{-3}$, which is the stoichiometric number of doped holes and which is in the range of what has been estimated from Hall measurements.[29] Using $m \simeq 3m_e$, consistent with specific-heat measurements,[30] we then estimate $E_f/h = 3270$ cm$^{-1}$. Since $\nu_0 = 540$ cm$^{-1}$ for the 6 K data, we fix the ratio $h\nu_0/E_f = 0.17$, i.e., we are in the adiabatic regime. Finally, we vary $U/E_f$ in the range 0.1–5. For values of $h\nu_0/E_f < 0.3$, the absorption shape is nearly independent of $U/E_f$, except that the magnitude of $\sigma_{\max}$ scales down with increasing $U/E_f$. For $U/E_f = 0.1$, we have $\sigma_{\max} = \alpha(2.37 \times 10^3)\ \Omega^{-1}\,\mathrm{cm}^{-1}$ which should fit the data with $\alpha$ of the order of 1.

For the considered frequency range above the threshold, we are always sufficiently close to the Fermi edge in order to approximate the frequency dependence of the imaginary part of the dielectric response by $(\omega - \omega_0)$, the number of excited low-energy particle-hole pairs. The scaling of the low-frequency slope (as suggested in Fig. 3) is implemented through the increase of the number of particle-hole pairs with increasing frequency (relative to the Fermi edge). The decrease at the high-energy side is controlled by a $1/\omega^3$ factor, most easily identified in the force-force correlation function form of the conductivity. Consequently, we expect the optical conductivity to approach

$$\sigma(\omega) \propto \left(\frac{\omega_0}{\omega}\right)^3 \left(\frac{\omega}{\omega_0} - 1\right). \tag{4}$$

Indeed, this formula matches the frequency dependence of the numerically calculated $\sigma(\omega)$ (solid line in Fig. 4). The model reproduces the observed shape of the polaron peak quite convincingly and it accounts for the scaling. However, it does not provide a mechanism for the observed shift of the threshold with temperature—which is probably controlled by the electron-phonon coupling strength. This necessitates to extend the considerations to intermediate or strong-coupling situations, first and foremost in the adiabatic limit. Such an evaluation is not available yet. It has to involve the collective response of the Fermi sea to the formation of a potential well during the absorption process which leads to singularities in the optical conductivity, well known from the x-ray edge problem. Recoil of the polaronic lattice deformation, which is taken up in the excitation process of the charge carrier to the Fermi edge,[31,32] flattens the singularity and might be responsible for the observed shape. Though the consequences for the shape of the absorption spectrum are speculative, the singular response is supposed to be present in any model with a sudden creation of a heavy or localized scatterer in the presence of a Fermi sea, and it will have to be investigated.

Apart from these considerations, the simple modeling presented above already characterizes the observed polaron excitations sufficiently well and we are in the position to identify the nature of the polaronic processes in LSMO and LCMO films as large and small polarons, respectively.

We acknowledge discussions with K.-H. Höck, T. S. Nunner, R. Hackl, A. Nucara, and P. Calvani. We thank J. Goldfuss and W. Westerburg for placing the samples at our disposal. The research was supported by BMBF (Grants Nos. 13N6917, 13N6918A) and partly by DFG through SFB 484 (Augsburg).

[1] R. von Helmolt *et al.*, Phys. Rev. Lett. **71**, 2331 (1993).
[2] P. Calvani, *Optical Properties of Polarons* (La Rivista del Nuovo Cimento, Bologna, 2001).
[3] D.C. Worledge *et al.*, J. Appl. Phys. **80**, 5158 (1996).
[4] Y. Okimoto *et al.*, Phys. Rev. B **55**, 4206 (1997).
[5] J.H. Jung *et al.*, Phys. Rev. B **57**, R11 043 (1998).
[6] K.H. Kim, J.H. Jung, and T.W. Noh, Phys. Rev. Lett. **81**, 1517 (1998).
[7] E. Saitoh *et al.*, Phys. Rev. B **60**, 10 362 (1999).
[8] H.J. Lee *et al.*, Phys. Rev. B **60**, 5251 (1999).
[9] S.G. Kaplan *et al.*, Phys. Rev. Lett. **77**, 2081 (1996).
[10] M. Quijada *et al.*, Phys. Rev. B **58**, 16 093 (1998).
[11] A. Machida, Y. Moritomo, and A. Nakamura, Phys. Rev. B **58**, R4281 (1998).
[12] H.G. Reik and D. Heese, J. Phys. Chem. Solids **28**, 581 (1967).
[13] M.J. Goovaerts, J.M. De Sitter, and J.T. Devreese, Phys. Rev. B **7**, 2639 (1973).
[14] D. Emin, Adv. Phys. **24**, 305 (1975).
[15] H. Röder, J. Zang, and A.R. Bishop, Phys. Rev. Lett. **76**, 1356 (1996).
[16] J.D. Lee and B.I. Min, Phys. Rev. B **55**, 12 454 (1997).
[17] A.J. Millis, R. Mueller, and B.I. Shraiman, Phys. Rev. B **54**, 5405 (1996).
[18] M.W. Kim *et al.*, Phys. Rev. Lett. **89**, 016403 (2002).
[19] D. Emin, Phys. Rev. B **48**, 13 691 (1993).
[20] J. Tempere and J.T. Devreese, Phys. Rev. B **64**, 104504 (2001).
[21] D. Christey and G. Hubler, *Pulsed Laser Deposition of Thin Films* (Wiley, New York, 1994).
[22] G. Jakob *et al.*, Phys. Rev. B **57**, 10 252 (1998).
[23] C. Hartinger, Ph.D. thesis, Universität Augsburg, 2002.
[24] H.G. Reik, in *Polarons in Ionic Crystals and Polar Semiconductors*, edited by J. Devreese (North Holland, Amsterdam, 1972).
[25] A.V. Puchkov *et al.*, Phys. Rev. B **52**, R9855 (1995).
[26] S. Yoon *et al.*, Phys. Rev. B **58**, 2795 (1998).
[27] P. Horsch, J. Jaklič, and F. Mack, Phys. Rev. B **59**, 6217 (1999).
[28] V. Gurevich, I. Lang, and Y. Firsov, Sov. Phys. Solid State **4**, 918 (1962).
[29] P. Mandal *et al.*, Phys. Rev. B **57**, 10 256 (1998).
[30] M.B. Salamon and M. Jaime, Rev. Mod. Phys. **73**, 583 (2001).
[31] J. Gavoret *et al.*, J. Phys. (Paris) **30**, 987 (1969).
[32] A.E. Ruckenstein and S. Schmitt-Rink, Phys. Rev. B **35**, 7551 (1987).